Validation of Inverter Labeling with Plant Transfer Functions

Joseph Ranalli
Penn State Hazleton
Hazleton, PA
jar339@psu.edu

***Abstract*—The large quantity of data sources found within a utility scale photovoltaic plant presents data quality control challenges. One potential issue is mislabeling of the plant's component outputs (e.g. production measurements made at the combiner or inverter level). If a component's output is incorrectly labeled, it presents an obstacle to plant monitoring and maintenance, as operators will not know where fixes are needed. This study aims to demonstrate the possibility of utilizing the Cloud Advection Model to perform quality checks on the labeling of production outputs at a plant component level based on information about the plant's spatial layout. Results utilizing simulated data showed that the plant transfer function predicted by the CAM could provide discrimination between plant segments that are separated in the cloud motion direction. The discrimination occurred primarily through the phase of the transfer function, but in cases where the spatial dispersion of the plant varied significantly in the cloud motion direction, changes to the transfer function bandwidth were also observable. This methodology shows promise using the simulated plant data in this study, which warrants further study and practical validation of this method utilizing real plant data.**

***Index Terms*—Variability, Data Validation, Cloud Advection Model**

I. Introduction

Efficient operation of utility scale photovoltaic (PV) plants requires the collection and handling of extremely large quantities of generation data that can be used to monitor the performance of the plant. These data can be used to assess plant component failures, damage, or other contingencies that impact the plant's overall generation, and thus, the economic return on the investment. Due to its importance, plant operators are regularly concerned about quality control for this data. One potential data quality issue is verification of correct labeling for all plant data sources. Specifically, the possibility exists that mistakes could be made during initial construction when labeling specific strings/combiners/inverters within the plant. Due to the large size of utility scale plants and the large number of labeled entities, performing audits would be a time consuming and cost intensive process that would require manual inspection of each component and its connections to the plant's data acquisition system. The present study simulates the use of variability models for performing a validation of data source location within an overall plant in an effort to provide an analytical method that would avoid this expense. The approach relies on the individual time series of plant sub-segment generation measurements and knowledge of the plant's layout.

II. Methodology

Since this paper only aims to demonstrate the feasibility of the concept, a distributed irradiance dataset was used to simulate the output of an actual plant, rather than utilizing real plant generation data. Different groupings of the individual sensors from the irradiance measurement network were used to simulate the various inverter segments of the plant. The previously described Cloud Advection Model (CAM) [1] was used to predict the output for each of the plant subsections based on its transfer function relative to a reference irradiance measurement. Comparing these predictions with the spatially aggregated irradiance measurement data allows interpretation to be made as to whether the segments were correctly labeled.

A. Cloud Advection Model

The Cloud Advection Model (CAM) was first proposed as a method to represent spatial aggregation of irradiance by a spatially distributed plant [1], [2] and served a similar purpose to the well-known Wavelet Variability Model (WVM) [3]. Where the WVM was derived to represent the effects of the aggregation process matched to long-term trends in variability, the CAM was shown to better represent aggregation in detail on short timescales when cloud advection dominates the variability [1].

The CAM models frozen advection of clouds over a hypothetical distributed plant by representing the plant as a transfer function with a low-pass filter characteristic. This transfer function has the effect of smoothing the irradiance time series. The transfer function defined by the CAM relates the frequency domain representation of a single reference point's irradiance time series, $G_{ref}(f)$, to the plant's aggregate irradiance, $P(f)$. Due to the convolutional nature of the frozen advection phenomenon, the form of this transfer function can be analytically derived and is written as the Fourier transform of the plant's 1-D spatial distribution, d^*, as in Eq. 1. For plants that are distributed over a two-dimensional area, the plant's spatial distribution can be projected into a 1-D form along the cloud motion vector, albeit with some degradation to the model's effectiveness [1].

$$TF(f) = \frac{P(f)}{G_{ref}(f)} = \mathcal{F}\left[d^*\left(\frac{x}{V_c}\right)\right] \quad (1)$$

B. Irradiance Data

The irradiance dataset used was that from the HOPE-Melpitz campaign [4]. The campaign utilized 50 distributed sensors that measured irradiance with a 1 second temporal resolution. Sensors were arranged into various groups in order to simulate the effects of the inverter or combiner arrangements within a hypothetical plant. Cloud advection speeds, V_c, are required as an input by the CAM, and were identified from the irradiance measurements using the method of Jamaly and Kleissl [5] on the entire field. The spatial distributions of the plant segments were computed by projecting the individual sensor positions onto the cloud motion vector as described previously.

III. Results and Discussion

The example calculation conducted in this study shows how this method might be applied for the purpose of verifying plant segment positions. Plant segments were defined within the irradiance measurement network, and transfer function predictions were computed using the CAM, relative to a common reference point. An example of selected plant component segments is shown in Fig. 1. The cloud motion vector for this plant was in the south-to-north direction, shown by the arrow in the figure. The aggregate outputs from the plant segments (shown on colored lines in Fig. 2) are similar and would be difficult to distinguish in the time domain. However, when computing transfer functions, differences arise that can be used to discriminate which segment is which. As seen in Fig. 3, the blue segment is observed to exhibit a rising phase, while green and blue both show falling phase. This results from the fact that blue is to the south of the reference point, causing its phase to lead the input. Conversely, the red and green signals are located north of the reference point and consequently lag the reference in time. The phase trends predicted by the CAM predictions match those found in the real data reasonably while coherence remains high, but fail to agree at higher frequencies.

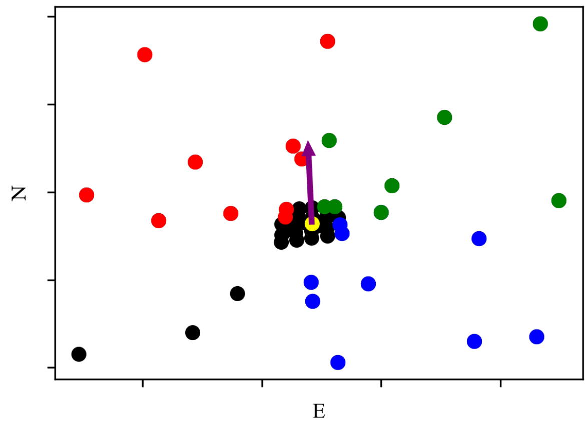

Fig. 1. Example plant layout. Yellow dot shows reference irradiance station. Red, Blue and Green sets of dots represent the two plant segments. Purple arrow shows south-to-north cloud motion direction.

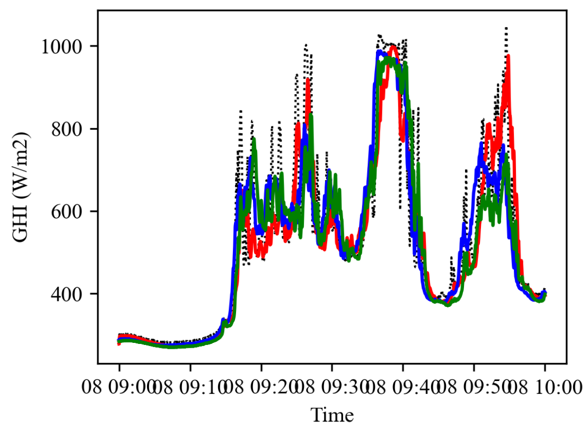

Fig. 2. Sample time series for the three plant subsets shown in in Fig. 1. Dashed line is the reference irradiance measurement.

Unlike the blue segment, the red and green segments in Fig. 1 are co-located with respect to the south-to-north cloud motion direction, and thus, have the same predicted phase behavior in Fig. 3. This prevents them from being differentiated on this basis. Attempts to fully map the plant therefore require investigation of multiple cloud motion directions that would induce spatial separation between the segments along the cloud motion vector. For example, using the same plant segments described in Fig 1, but instead focusing on a time period where the clouds move from west-to-east, different transfer functions behavior can be obtained, shown in Fig 4. In this case the red segment exhibits leading delay in the phase (due to its position west of the reference), while blue and green have indistinguishable lagging phase due to their similar eastward position.

Unlike the phase, the magnitude does not provide a clear discriminator between the segments for the previous examples. In part, this is due to the fact that when segments have the same projected size and shape in the cloud motion direction, the CAM's physical basis would lead to prediction of identical transfer function magnitude shapes. In this case, all plant segments described in Fig. 1 have similar spatial distributions and extents relative to the cloud motion directions tested, so it is unsurprising that their predicted and measured transfer function magnitudes are similar. On the other hand, for plant segments with different spatial extents in the cloud motion direction (e.g. in Fig. 5), the bandwidth does provide some discrimination capability. As seen in Fig. 6, the blue segment exhibits a higher bandwidth, resulting from its more compact size relative to the cloud motion and its reduced effect at smoothing the variability. This result is also predicted by the output of the CAM model. As before, the phase characteristics also provide discrimination between these two segments due to their spatial separation along the cloud motion direction.

Some discussion is warranted on the impact of the temporal resolution of the data. Though the low-frequency phase provides the clearest discrimination of the phase delay difference between the plant segments, it is necessary that the sampling

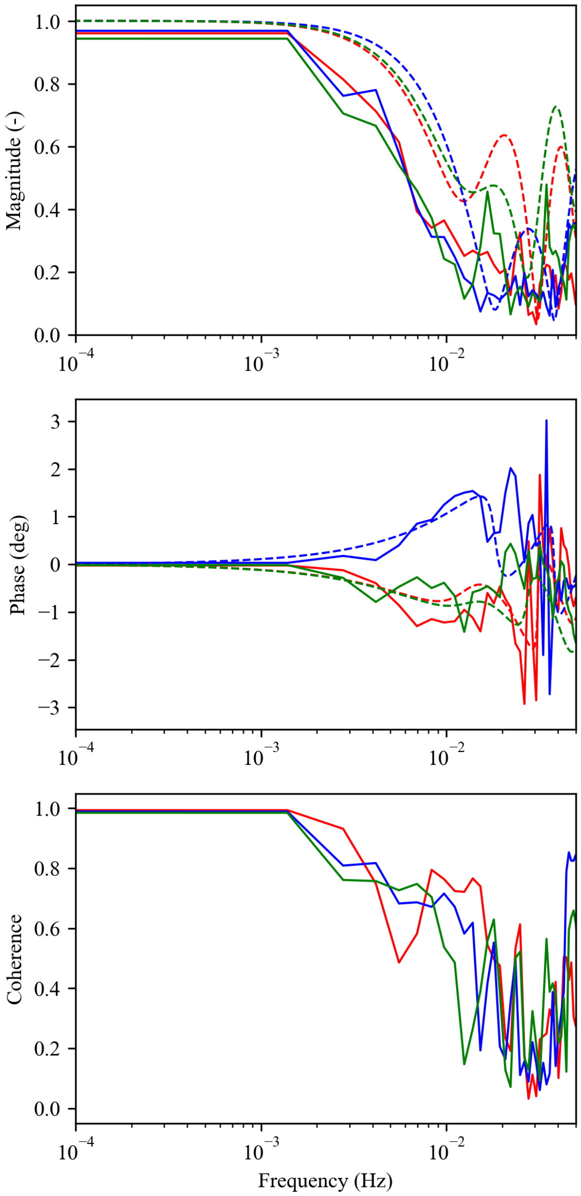

Fig. 3. Transfer functions for the plant subsets show in in Fig. 1. Dashed line is the CAM model prediction for each segment.

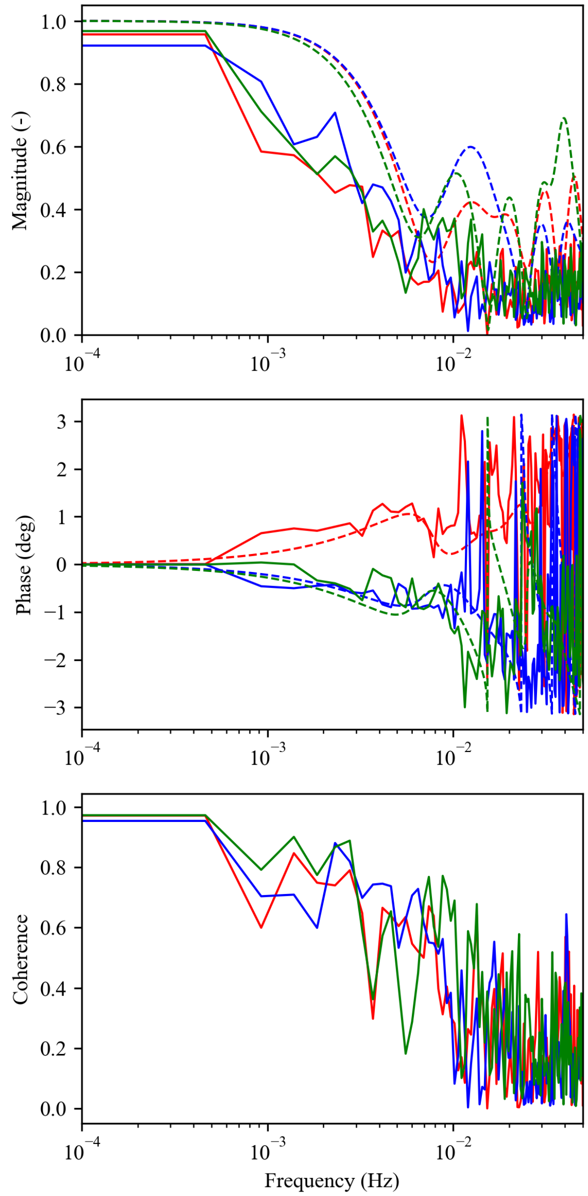

Fig. 4. Transfer functions for the same plant subsets shown in in Fig. 1, but for a different time period with a west-to-east cloud motion. Dashed line is the CAM model prediction for the segments.

rate for the data is high enough to actually capture the temporal delay between the signals. Delay can be imagined as proportional to the segments' spatial separation distance along the cloud advection direction and inversely proportional to the cloud motion speed. In the case of the south-to-north cloud motion, the midpoint separation between the red and green segments in Fig. 1 was approximately 1 km, with cloud motion speeds of around 20 m/s, corresponding to an expected delay of approximately 50 seconds between the two segments. The 1 second resolution data used in this study was therefore sufficient to resolve this delay, but 1 minute or 5 minute resolution data might be sampled too slowly to meaningfully observe the difference.

IV. Conclusion

This study demonstrated the feasibility of using the previously reported Cloud Advection Model (CAM) for matching of the transfer function between a plant segment and a reference irradiance measurement. This approach is proposed as a method to cross-check the accurate labeling of plant segments (e.g. inverter- or combiner-level outputs) within a larger PV plant.

The results showed that the transfer function appears to provide some discrimination of the position of sub-plant segments. The transfer function phase provides a more consistent representation of the location of the segment, as compared

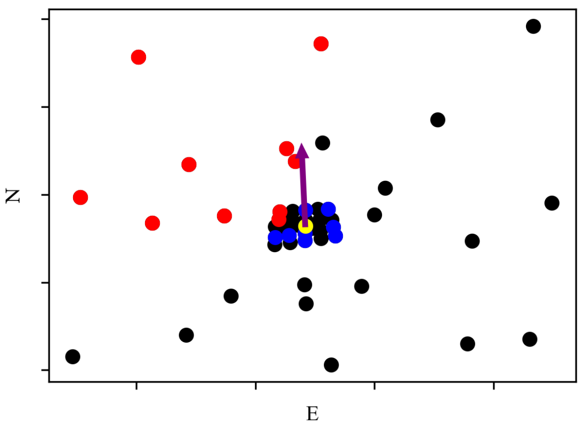

Fig. 5. Layout of plant with different spatial dispersion in the cloud motion direction. Yellow dot shows reference irradiance station. Red and Blue dots represent the two plant segments. Green arrow shows cloud motion direction.

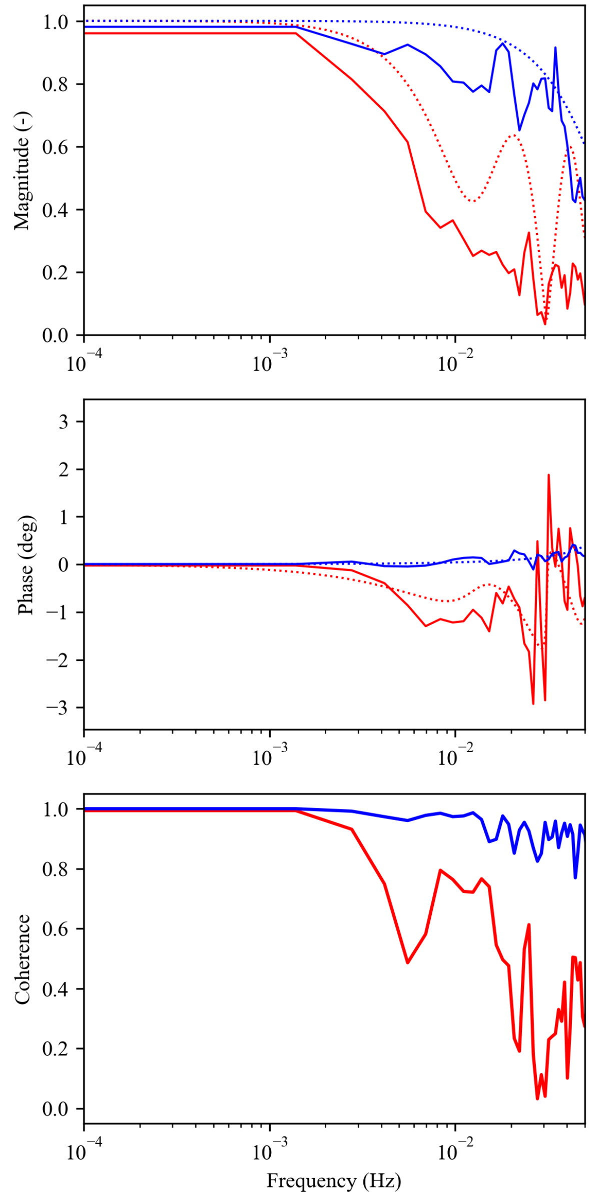

Fig. 6. Transfer functions for the two plant subsets shown in in Fig. 5. Dashed line is the CAM model prediction for the segment.

to the transfer function magnitude. This results from the fact that the phase characteristics are dominated by the group delay, which was apparent when considering segments with a spatial separation in the cloud motion direction. The delay between these segments was matched reasonably well by the CAM model at low frequencies, where the coherence between the signals remained relatively high. Due to the advective physics dominating these relationships, it was observed that discrimination of segment position within the field is difficult when working with segments that are co-located with respect to the direction of the cloud motion. However, the ability to discriminate those segments was regained by considering additional time periods with perpendicular cloud motion directions (i.e. aligned with the spatial separation between the plant segments).

The bandwidth inferred from the transfer function magnitude was observed to provide some discriminatory capability when considering two plant segments with different aspect ratios or orientations with respect to the cloud motion direction. However, detailed dynamical characteristics of the transfer function magnitude were too noisy to be matched effectively by the model, due to the loss of coherence. Thus, the transfer function magnitude seems unlikely to provide a good target for identifying plant segments, unless a high degree of non-uniformity is present within the plant segment configurations.

Some limitations of the method can be inferred from the present work. Implementing this analysis requires temporally coincident data from the various site segments along with some indication of the cloud motion vector. Such time periods require data with moderate variability induced by consistent cloud motion, such that the frozen cloud advection assumption of the CAM is satisfied. In order to map a full two-dimensional plant, it is necessary to investigate multiple such time periods with sufficiently perpendicular cloud motion vector components. It is also necessary for the generation data to be sampled at a sufficiently high rate to resolve the temporal delay between segments.

While the present results indicate that this method shows promise for plant quality control applications, this demonstration was based on distributed irradiance sensor data, rather than actual outputs from a plant. Future work would be needed to test this method on real plant data to determine its effectiveness for practical applications and its suitability for quality control in a real setting. Additionally, automation of this process would be desirable to facilitate its adoption across an entire utility scale PV plant.

V. Acknowledgment

The author would like to acknowledge financial support from Penn State Hazleton and the Penn State School of Engineering Design and Innovation.

References

[1] J. Ranalli and E. E. M. Peerlings, "Cloud advection model of solar irradiance smoothing by spatial aggregation," *Journal of Renewable and Sustainable Energy*, vol. 13, no. 3, p. 033704, May 2021, publisher: American Institute of Physics. [Online]. Available: https://aip.scitation.org/doi/abs/10.1063/5.0050428

[2] J. Ranalli, E. E. Peerlings, and T. Schmidt, "Cloud Advection and Spatial Variability of Solar Irradiance," in *47th IEEE Photovoltaic Specialist Conference (PVSC)*. Virtual: IEEE, Jun. 2020, p. 8.

[3] M. Lave and J. Kleissl, "Cloud speed impact on solar variability scaling – Application to the wavelet variability model," *Solar Energy*, vol. 91, pp. 11–21, May 2013. [Online]. Available: http://www.sciencedirect.com/science/article/pii/S0038092X13000406

[4] A. Macke, P. Seifert, H. Baars, C. Barthlott, C. Beekmans, A. Behrendt, B. Bohn, M. Brueck, J. Bühl, S. Crewell, T. Damian, H. Deneke, S. Düsing, A. Foth, P. D. Girolamo, E. Hammann, R. Heinze, A. Hirsikko, J. Kalisch, N. Kalthoff, S. Kinne, M. Kohler, U. Löhnert, B. L. Madhavan, V. Maurer, S. K. Muppa, J. Schween, I. Serikov, H. Siebert, C. Simmer, F. Späth, S. Steinke, K. Träumner, S. Trömel, B. Wehner, A. Wieser, V. Wulfmeyer, and X. Xie, "The HD(CP)^2 Observational Prototype Experiment (HOPE) – an overview," *Atmospheric Chemistry and Physics*, vol. 17, no. 7, pp. 4887–4914, Apr. 2017. [Online]. Available: https://www.atmos-chem-phys.net/17/4887/2017/acp-17-4887-2017-discussion.html

[5] M. Jamaly and J. Kleissl, "Robust cloud motion estimation by spatio-temporal correlation analysis of irradiance data," *Solar Energy*, vol. 159, pp. 306–317, Jan. 2018. [Online]. Available: http://www.sciencedirect.com/science/article/pii/S0038092X17309556